BLSML: A Combined Passive Method for Target Position Estimation using Brown's Least Square Error and Maximum Likelihood with Integrated Optimization

Mahmood (Kamran) Mohammadzadeh
School of Electrical Engineering, Shahrood University of technology, Shahrood, Iran
Mhmdzdh1@gmail.com

***Abstract*—This paper presents the BLSML method, which combines Brown's Least Square Error (LSE) and Maximum Likelihood (ML) techniques for accurate target position estimation. The proposed method, named BLSML, offers a passive approach that leverages the strengths of both LSE and ML to improve the estimation accuracy. In the first stage, BLSML provides an initial estimated position using LSE, which takes advantage of the robustness and efficiency of the LSE algorithm. Then, in the second stage, BLSML performs optimization based on ML principles, refining the estimated position to enhance accuracy. We have utilized the Cramer-Rao Lower Bound (CRLB) on the estimator's covariance to develop an efficient estimator for position estimation. To assess the performance of the proposed BLSML method, comprehensive Monte Carlo simulations were conducted. Realistic noise and error models were incorporated to mimic real-world conditions and evaluate the method's robustness. The evaluation metrics included Root Mean Square Error (RMSE) for position estimation accuracy and Circular Error Probable (CEP) for error region analysis. The results demonstrated that BLSML achieved remarkable accuracy, with an RMSE below 0.43%, an average estimation error of 1.907% and the radius of the 90% CEP region of approximately 925 m for target position estimation within a 200-kilometer range.**

***Index Terms*— Maximum likelihood estimation, Transmitting or emitting target position estimation, LSE-Brown, BLSML, Optimization, AoA.**

I. INTRODUCTION

Determining the location of emitting targets is a critical task performed by communication *electronic warfare* (EW) systems. The knowledge of target locations serves multiple purposes. Firstly, it provides valuable insights into the positioning and distribution of forces, enabling a better understanding of the overall military situation. Secondly, precise target location information facilitates the effective utilization of advanced weaponry, such as GPS-enabled fire-and-forget munitions, which can accurately engage and neutralize the identified targets. Lastly, when different types of emitters are clustered in a specific region, it can provide indications about the presence and nature of particular entities at that location.

There are several methods to estimate the azimuth *angle of arrival* (AoA) of signals impinging on the antenna array at an intercept site. such as *time difference of arrival* (TDoA), *time of arrival* (ToA), *range differences* (RD), *differential Doppler* (DD) [1].

All of these techniques generate quadratic curves, called *lines of bearing* (LoB), upon which the emitter lies, subject to measurement errors and noise perturbations. The intersection of these LoBs is used to estimate the *position fix* (PF) of a target. If the target is moving, errors can occur in the PF calculations. These errors can be mitigated if the motion is detected [1].

The AoA of a signal, or its LoB, is a frequently used parameter for PF computation. Two or more LoBs, assumed to be measured on the same target at more or less the same time, may intersect [2-7]. Such a technique for PF determination is referred to as *triangulation*.

In Fig. 1., the components related to the BLSML target estimation method are depicted. In this scenario, the drone follows a pre-determined path, the mounted receiver on the drone, along with the radar transmitter, forms a system. The target's LoBs, which exists in two types: *line of sight* (LoS) and *non-line of sight* (NLoS), is received by the receiver. After relevant processing, the position of the transmitting or emitting target is determined using the BLSML method, which involves statistical, trigonometric, and optimization computations.

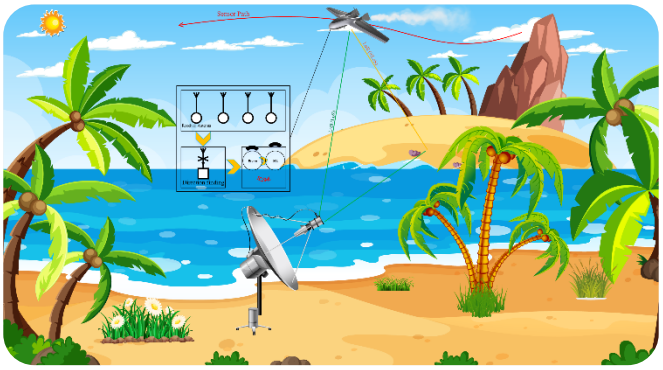

Fig. 1. The components of the BLSML method for target position estimation.

A. Previous Literature

The recursive form of LSE estimation is assumed such that measurements are made sequentially at different times. LSE estimation can be applied to any appropriate set of data points. The linear estimation model is an expression consisting of the observation matrix and unknown parameters [7].

When noise is present in observation matrix, the estimation isn't optimal. It exhibits bias and increased covariance. To determine the optimal LSE estimate in this case, the method of *Total Least-Squares Estimation* (TLSE) was developed [8].

In general, the LSE estimation process produces biased estimates. The term biased estimator for the parameter θ means that $E[estimator] \neq \theta$. The symbol $E[\cdot]$ indicates the expectation operation [9].

However, specific cases of LSE estimation, can produce unbiased results. An algorithm developed by Brown [10] based on an earlier algorithm by Legendre [11] presented for calculating the PF, which

is based on minimizing the square of the miss distance of the PF from the measured LoBs. This algorithm was presented in [3] also.

A different LSE estimation that called Hemispheric for PF estimation is presented in [12, 13]. The measured bearing from a sensor, φ_i projected onto the surface of the Earth in the northern hemisphere. A problem with this LSE approach to PF is that an initial estimate of the target is required and it is only valid for small bearing errors. Also, convergence is not guaranteed and slow convergence may occur even when convergence occurs.

In [14-21], the position estimation of an emitter has been performed using the ML method.

In [14], a method for estimating various target parameters, including range, is investigated using an active approach. The method used is called *joint estimation of velocity, AoA, and range* (JEVAR), which takes into account multipath in the environment and employs ML estimation in the receiver part. Their proposed method has shown better performance compared to other methods and achieved range estimation with centimeter-level accuracy.

In [15], an ML estimator is used to estimate the position of an emitter or a radio wave source using UAVs in NLoS environments. Each receiver sensor measures the *direction of arrival* (DoA). In their method, after estimating the source's position, it is determined which measurements are LoS or NLoS, and then the position estimation is corrected accordingly. Multiple UAVs are used for measurements to improve accuracy and coverage. We have also measured only the AoA in order to reduce complexity.

In [16], they have used ML receivers to determine the position of an emitter for radar pulse trains. In the method they developed, they have eliminated the need for a complex antenna array and synchronization. They have utilized a sensor for measuring ToA. In the first stage, they model the localization problem as a *nonlinear least square* (NLS) problem from the perspective of ML estimation. Finally, they propose an iterative estimation algorithm for accurate emitter position estimation. Similar to this work, we have utilized a two-stage method where the second stage is iterative.

In [17], a method for target localization using *wireless sensor networks* (WSNs) in terrestrial and underwater environments is proposed. Their proposed method consists of several components: ML receiver sensors, a data transmission component for collecting data from the sensors, and a position estimation algorithm operator. The collected data from the sensors in this work can be selected by the user to be any of AoA, ToA, TDoA, and *received signal strength* (RSS), based on the desired accuracy of position estimation and computational complexity. Additionally, they have developed algorithms for position estimation using triangulation, trilateration, and multilateration methods.

In [18], similar to the approach in [14], they have used an active method for moving target localization. The developed method by them is comparable to other methods in terms of the time required to achieve accurate position estimation. They have achieved this by reducing computational complexity. Indeed, their estimation error is high at low *Signal-to-Noise Ratio* (SNR) levels, and they also face challenges in reaching the CRLB even at high SNR. In this work, achieving sufficient accuracy within a reasonable time was one of their concerns, which is also a concern we have encountered.

Based on the conducted investigations, we have concluded that we can utilize a passive approach for our work.

In [19, 20, 22], they have utilized the combination of different received data for target estimation. In [19], ML receivers simultaneously measured RSS and ToA.

In [20], a proposed position estimation method is introduced, specifically designed for crowded urban environments, aiming to reduce the reliance on LoS paths. In their proposed method, they have utilized a combination of different received data, including ToA and AoA. Additionally, they have defined a motion path for the platform. In our proposed method, we have the flexibility to have multiple measurements by employing multiple UAVs or, similar to the approach in [20], defining a specific path for a single UAV to traverse. In our case, we have chosen to utilize the second approach.

In [21], a cost function has been proposed to handle noisy measurements and solution of unknown parameter.

In [22], a heterogeneous dataset comprising TDoA, RSS and AoA measurements is collected using a multi-sensor system. Then, a set of regression-based methods is employed to estimate the position of an emitter.

There are several sources of error that can enter into the PF estimation by triangulation: noise and measurement errors. In [23], an analysis of sensor position error effects on the estimation of three-dimensional target has been conducted.

B. Motivation and Contribution

Based on our conducted investigations, we have concluded that we can utilize a passive approach. In order to reduce computational complexity, we consider the AoA and sensor position as data in each measurement, which is one of the strengths of our proposed method. Furthermore, it was concluded that defining a specific path for the drone and having it traverse that path while simultaneously performing measurements and target position estimation using BLSML method.

A summary comparison of the methods introduced here is provided in Table I.

TABLE I

COMPARISON OF THE DISCUSSED POSITION ESTIMATION METHODS.

Method	Biased	Iterative
LSE-Brown	*No*	*No*
LSE-Hemispheric	*No*	*Yes*
ML	*No*	*Yes*

The contributions of this work include the following:

1) The development of the BLSML method that consists of two distinct stages: initial position estimation and optimization of the estimated position. In the first stage, we employ the Brown-LSE method to estimate the initial position. The LSE-Brown method is known for its robustness and efficiency in providing reliable initial position estimates. Unlike some other methods that require iterative procedures, the LSE-Brown method offers a powerful and non-iterative approach for determining the initial position. This initial estimation serves as a starting point for further optimization. The second stage of the BLSML method involves optimization of the estimated position using the ML approach. By employing ML optimization, we refine the initially estimated position to enhance accuracy and precision. Compared to the LSE-Hemispheric method, the ML approach demonstrates faster convergence and increased stability during the optimization process.

2) In the simulation, various measurement errors and noises have been considered. The defined noises and errors are assumed AWGN with a mean of zero except for the NLoS measurements, which we have considered to follow a Rayleigh distribution. The standard deviations of these noises and errors are different. The error in determining the drone's position using GPS is assumed to have a standard deviation of 5 meters. The standard deviation of LoB measurement is considered to be 1 degree. The error due to the drone's motion is assumed to have a standard deviation of 0.5 degrees. The NLoS measurements has a standard deviation that is 3.5 times the standard deviation of the RMS of aforementioned noises. Because up to 3 times the standard deviation of the defined RMS noise [24] is considered as acceptable noise levels. It also includes 5% of the measurements.
3) In order to execute the BLSML method for target position estimation, it is necessary to determine the initial LoB for position estimation. This is because the estimation error is significantly high for positions estimated at the beginning of the drone's motion. This is primarily due to the requirement of a sufficient number of measurements for the ML algorithm to provide accurate position estimation [25]. To determine the initial LoB, we have used RMSE. In the Monte Carlo simulations, the drone has followed the predefined path for 1000 iterations, and the RMSE value has been calculated. And we have determined the initial LoB for the RMSE of 10%, 5% and 1%. The first view by the drone has been considered between -5 degrees and -45 degrees. After the iterative process, where the first LoB consisted of several angles between -5 degrees and -45 degrees, an interpolation has been performed. The interpolation process aims to determine the LoBs that achieve an RMSE value below 10% error. Also, the interpolation has been performed with an accuracy of 0.1 degrees. Based on the first view by the drone, the position estimation process is initiated by determining the LoB according to the described curve. The curve has also been obtained for RMSE values of 5% and 1%.
4) Measurement errors and noises include the following cases: LoB measurement error, drone positioning measurement error, drone movement error along the specified path, *non-line of sight* (NLoS) measurements, and noise related to changes in drone velocity such as environmental factors like weather, which are considered during the time intervals between measurements.
5) Simulation of removing NLoS measurements by utilizing the difference between the estimated target LoB and the current LoB.
6) Monte Carlo simulation of the BLSML method and its evaluation using RMSE, *Cumulative Distribution Function* (CDF) [26] and CEP.

The rest of the paper is organized as follows. The system model for this work, which involves the position estimation method using the BLSML method, is introduced in Sec. II, the derivatives of the CRLB are explained in Sec. III, Sec. IV presents the simulation results, and finally the paper is concluded in Sec. V.

II. System Model

Fig. 2. illustrates an example of system model for target position estimation using BLSML method. The block diagram shown consists of three parts: the radar transmitter, depicted in Fig. 2. (a), which radiates the signal into space. The radar receiver, shown in a lighter shade in Fig. 2. (b), which is a type of superheterodyne receiver in this case, receives the $signal + noise\ and\ interference$. Furthermore, these are received by the receiver mounted on the identification drone, shown in Fig. 2. (c).

The receiver mounted on the identification drone in Fig. 2. (c) comprises various components. A low-noise RF amplifier performs the amplification and filtering operations. The next block is related to signal identification and interference rejection. This block can be implemented using various methods, including deep learning, to retain only the signal and eliminate interference generated by other systems present in the environment. The direction finding block focuses on determining the AoA with a specific accuracy using different methods, such as DoA. After determining the AoA, the BLSML block applies the proposed method to estimate the radar position.

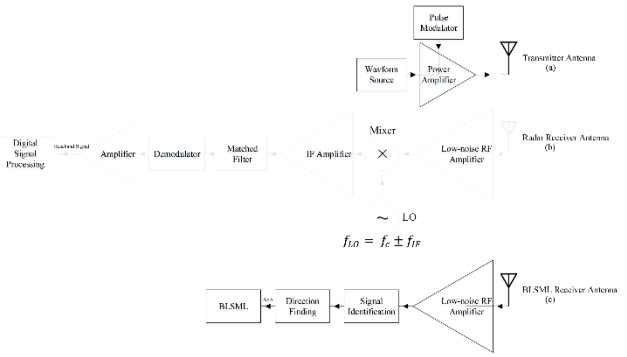

Fig. 2. (a) The radar transmitter, which is the transmitting target in this case. (b) Radar receiver which is a type of superheterodyne receiver. (c) The receiver mounted on the identification drone where the BLSML method is applied.

A. Initial Estimate

As mentioned, in this research, we have used the LSE-Brown method to determine the initial estimate of the target.

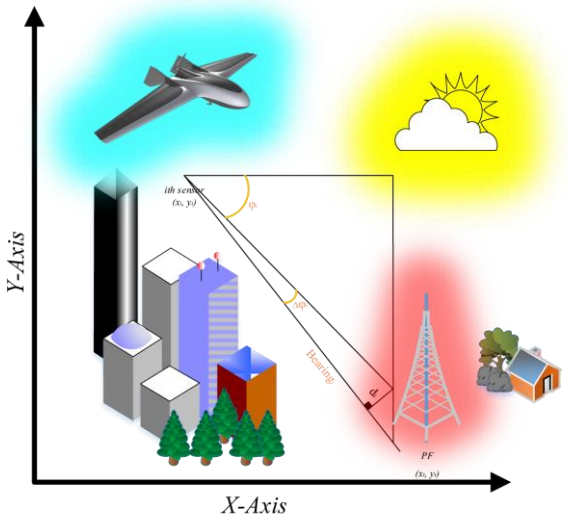

Fig. 3. LSE-Brown method.

This approach relies on minimizing the squared difference between the estimated position of the PF and the measured LoBs [10]. With reference to Fig. 3., to minimize the sum of the squares of the total miss distance, formulate

$$D = \sum_{i=1}^{N} d_i^2 = \sum_{i=1}^{N} a_i^2 x_T^2 + \sum_{i=1}^{N} 2a_i b_i x_T y_T - \sum_{i=1}^{N} 2a_i c_i x_T + \sum_{i=1}^{N} b_i^2 y_T^2 - \sum_{i=1}^{N} 2b_i c_i y_T + \sum_{i=1}^{N} c_i^2 \quad (1)$$

where

$$a_i = \sin\varphi_i$$

$$b_i = -\cos\varphi_i$$

$$c_i = x_i \sin\varphi_i - y_i \cos\varphi_i$$

N is the number of LoBs.

By equating the first partial derivatives of D with respect to x_T and y_T to zero, the values of x_T and y_T can be determined at which the total squared distance is minimized.

$$\frac{\partial D}{\partial x_T} = 0 = 2x_T \sum_{i=1}^{N} a_i^2 + 2y_T \sum_{i=1}^{N} a_i b_i - 2\sum_{i=1}^{N} a_i c_i \quad (2)$$

$$\frac{\partial D}{\partial y_T} = 0 = 2x_T \sum_{i=1}^{N} a_i b_i + 2y_T \sum_{i=1}^{N} b_i^2 - 2\sum_{i=1}^{N} b_i c_i \quad (3)$$

which yield

$$x_T = \frac{\sum_{i=1}^{N} b_i^2 \sum_{i=1}^{N} a_i c_i - \sum_{i=1}^{N} a_i b_i \sum_{i=1}^{N} b_i c_i}{\sum_{i=1}^{N} a_i^2 \sum_{i=1}^{N} b_i^2 - (\sum_{i=1}^{N} a_i b_i)^2} \quad (4)$$

$$y_T = \frac{\sum_{i=1}^{N} a_i^2 \sum_{i=1}^{N} b_i c_i - \sum_{i=1}^{N} a_i b_i \sum_{i=1}^{N} a_i c_i}{\sum_{i=1}^{N} a_i^2 \sum_{i=1}^{N} b_i^2 - (\sum_{i=1}^{N} a_i b_i)^2} \quad (5)$$

The aforementioned miss distance for sensor i can be represented as follows.

$$d_i = a_i x_T + b_i y_T - c_i \quad (6)$$

If we consider i as the index of the ith measurement of a LoB, and a_i, b_i, and c_i are as provided earlier, then the expression for the miss distance can be written in matrix form as follows.

$$\vec{d} = H\overrightarrow{x_T} - \vec{c} \quad (7)$$

In this expression,

$$\vec{c} = \begin{bmatrix} c_1 \\ \vdots \\ c_N \end{bmatrix} \quad \overrightarrow{x_T} = \begin{bmatrix} x_T \\ y_T \end{bmatrix} \quad H = \begin{bmatrix} a_1 & b_1 \\ \vdots & \vdots \\ a_N & b_N \end{bmatrix} \quad \vec{d} = \begin{bmatrix} d_1 \\ \vdots \\ d_N \end{bmatrix} \quad (8)$$

equation (9) provides the formula for calculating the LSE estimator of the target location vector $\overrightarrow{x_T}$

$$\overrightarrow{x_T} = [H^T H]^{-1} H^T \vec{c} \quad (9)$$

B. Optimization

As mentioned before, after estimating the target position using LSE-Brown, we have used the ML method to optimize the estimated position.

If we assume that the noise follows a Gaussian distribution with a mean of zero, the ML estimator for the target location can be expressed as follows:

$$\hat{\vec{x}} = \underset{\vec{x}}{\operatorname{argmin}}\, F(\vec{x}.\vec{\varphi}) \quad (10)$$

where

$$F(\vec{x}.\vec{\varphi}) = \frac{1}{2}[\vec{g}(\vec{x}) - \vec{\varphi}]^T C_{xx}^{-1} [\vec{g}(\vec{x}) - \vec{\varphi}] \quad (11)$$

The cost function, denoted as $F(\vec{x}.\vec{\varphi})$, consists of several components

$$\vec{g}(\vec{x}) = [g_1(\vec{x}) \cdots g_N(\vec{x})]^T \quad (12)$$

In two dimensions,

$$\vec{x} = [x_T \; y_T]^T \quad (13)$$

and the bearing measurements are given by

$$\vec{\varphi} = [\varphi_1 \cdots \varphi_N]^T \quad (14)$$

The components of $\vec{g}(\vec{x})$ are given by

$$g_n(\vec{x}) = tan^{-1}(\frac{\Delta_{y_n}}{\Delta_{x_n}}) \quad (15)$$

where

$$\Delta_{x_n} = x_T - x_n \quad . \quad \Delta_{y_n} = y_T - y_n \quad (16)$$

In conclusion, the covariance matrix C_{xx}, which has dimensions $N \times N$, represents the diagonal matrix $diag(\sigma_1^2 \cdots \sigma_N^2)$ and contains the variances of the N LoB observations.

N represents the total number of observations, and it is possible for multiple observations to be obtained from each sensor. However, it is assumed that the number of observations remains consistent across all sensors. The LoB observations are affected by AWGN given by

$$\delta\vec{\varphi} = [\delta\varphi_1 \cdots \delta\varphi_N]^T \quad (17)$$

If we denote the true LoB values as $\overrightarrow{\varphi_0}$, the observed LoBs can be represented as:

$$\vec{\varphi} = \overrightarrow{\varphi_0} + \delta\vec{\varphi} \quad (18)$$

Expression (11) can be put in the form

$$F(\vec{x}.\vec{\varphi}) = \frac{1}{2}\vec{f}^T C_{xx}^{-1} \vec{f} = \frac{1}{2}\sum_{n=1}^{N} \frac{f_n^2}{\sigma_n^2} \quad (19)$$

where

$$\vec{f} = [f_1 \cdots f_N]^T = \vec{g}(\vec{x}) - \vec{\varphi} \quad (20)$$

The numerical solution of (10), which is a nonlinear equation, can be obtained using the Newton-Gauss method. This iterative method allows us to find a solution by performing successive iterations until a desired level of convergence is achieved.

$$\hat{\vec{x}}_{m+1} = \hat{\vec{x}}_m + [\vec{g}_x^T C_{xx}^{-1} \vec{g}_x]^T \vec{g}_x^T C_{xx}^{-1} [\vec{\varphi} - \vec{g}(\hat{\vec{x}}_m)] \quad (21)$$

where $\vec{g}_x = \frac{\partial \vec{g}}{\partial \vec{x}}$ evaluated at the true target position, yielding

$$\vec{g}_x = \begin{bmatrix} \frac{-\Delta_{y_1}}{d_1^2} & \cdots & \frac{-\Delta_{y_N}}{d_N^2} \\ \frac{\Delta_{x_1}}{d_1^2} & \cdots & \frac{\Delta_{x_N}}{d_N^2} \end{bmatrix} \quad (22)$$

with

$$d_n^2 = \Delta_{x_n}^2 + \Delta_{y_n}^2 \quad (23)$$

C. NLoS Suppression

Also, we have proposed a method for suppression measurement errors caused by NLoS, inspired by the approach described in [27].

In this method, we calculate the difference between the current LoB and the current line to the estimated point. If the difference exceeds 5 degrees, it is considered as NLoS measurement and not included in the target's position estimation.

III. CRLB

In this section, we will discuss the derivatives of the CRLB as a measure of the efficiency of an estimator for the unknown parameter.

For an unbiased estimator $T(x)$ for the unknown parameter θ based on observations of the random variables $x_1.x_2.\cdots.x_n$ and with the joint probability density function $f(x;\theta)$, we have:

$$E[T(x) - \theta] = \int_{-\infty}^{\infty}(T(x) - \theta)f(x;\theta)dx = 0 \tag{24}$$

By simplifying this expression, it can be proven that

$$Variance\big(T(x)\big) \geq -\frac{1}{E[\frac{\partial^2 \log f(x;\theta)}{\partial\theta^2}]} \tag{25}$$

If the random variables $x_1.x_2.\cdots.x_n$ are *independent, identically distributed* (i.i.d), then

$$\log f(x;\theta) = \sum_i f(x_i;\theta) \tag{26}$$

And the CR bound is given by

$$Variance\big(T(x)\big) \geq -\frac{1}{nE[\frac{\partial^2 \log f(x_i;\theta)}{\partial^2\theta}]} \tag{27}$$

In this case, the unbiased estimator $T(x)$ with the lowest possible variance is said to be an efficient estimator for θ. In general, such an estimator may or may not exist and it depends on the situation at hand. It can be proven that if an efficient estimator exists, it will be the ML estimator.

In equation (25), the value of *fisher information* (FI) available in the dataset about the parameter θ is given by the following equation [9].

$$FI = -E[\frac{\partial^2 \log f(x;\theta)}{\partial\theta^2}] \tag{28}$$

In this work, we have derived the equations associated with the ML estimator through the equations mentioned in this section.

IV. Simulation Results

In this section, we will discuss the results obtained from Monte Carlo simulations of the developed method.

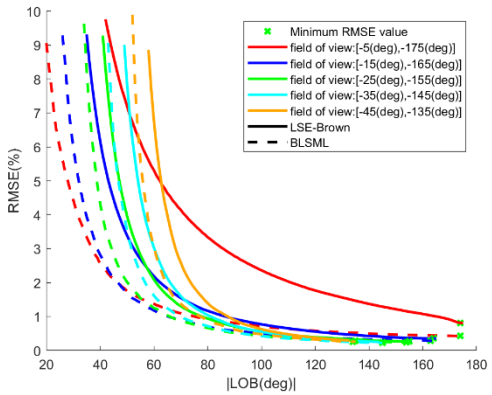

Fig. 4. Comparison between the LSE-Brown and BLSML methods in different FoVs.

Fig. 4. illustrates the RMSE plots for the LSE-Brown and BLSML methods across several *field of views* (FoVs).

It is evident that the BLSML method reaches an RMSE of 10% much faster. It is worth mentioning that the starting point for all the plots represents a 10% RMSE. Additionally, the lowest RMSE is achieved at the last view.

The Monte Carlo simulations between BLSML and LSE-Brown in terms of the time taken to reach a 10% RMSE is shown in Fig. 5. From the results of Fig. 5., it can be concluded that when the first view has a larger size, the time taken to reach a 10% RMSE is shorter, and vice versa. The reason for this is that in smaller-sized views, the sensor and target are almost aligned on a straight line, which leads to higher errors [25].

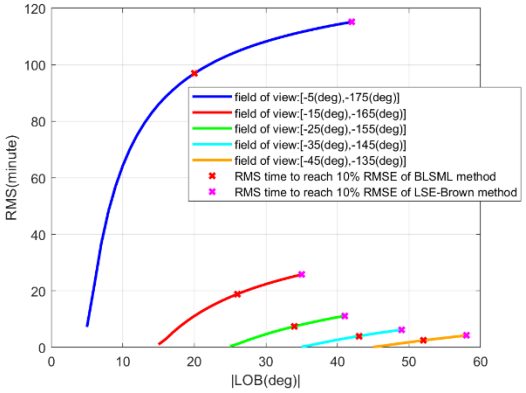

Fig. 5. Comparison of the time taken to reach 10% RMSE in the LSE-Brown and BLSML methods.

One of the additional evaluations we performed for the BLSML method is the calculation of the CDF based on the RMSE of the position estimation. In Fig. 6., we have presented the Monte Carlo simulation of the CDF for a target within a range of 200 kilometers.

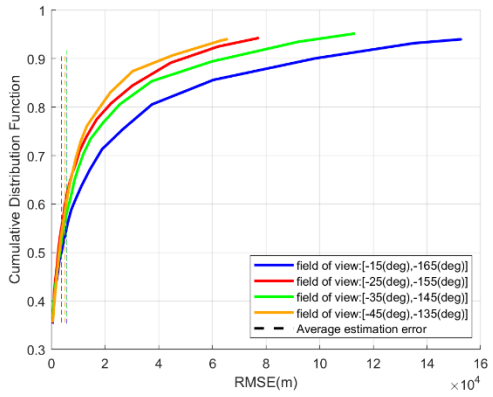

Fig. 6. The CDF of target position estimation using the proposed method for a number of FoVs. The simulations were iterated 1000. The best average estimation error was obtained in the FoV ranging from -25 degrees to -155 degrees.

The average RMSE values for the BLSML method for different FoV are provided in Table II. In Table III, a comparison of the

average RMSE of the position estimation with other methods is presented. Based on Table III our proposed method has shown a better average RMSE compared to the other two methods. It should be noted that in the two methods we compared, as the distance from the target to the origin of the coordinate system was not specified, we considered the maximum possible value within their defined region to ensure the best results.

TABLE II

THE AVERAGE RMSE OF BLSML FOR DIFFERENT FOVS.

FoV(DEG)	Average RMSE(m)
[-15,-165]	*5718.2*
[-25,-155]	*3813.91*
[-35,-145]	*5672.29*
[-45,-135]	*5153.63*

TABLE III

THE PROPOSED METHOD IS COMPARED TO OTHER METHODS IN TERMS OF AVERAGE RMSE, CONSIDERING THE CDF. THE CORRESPONDING FOV FOR THE PROPOSED METHOD IS [-25(DEG), -155(DEG)].

Method	Average RMSE(%)
[15]	*2.308*
BLSML	***1.907***
[20]	*7.955*

Fig. 7. illustrates another comparison showing the RMSE value based on the number of sensor measurements. This figure presents the Monte Carlo simulation of this evaluation.

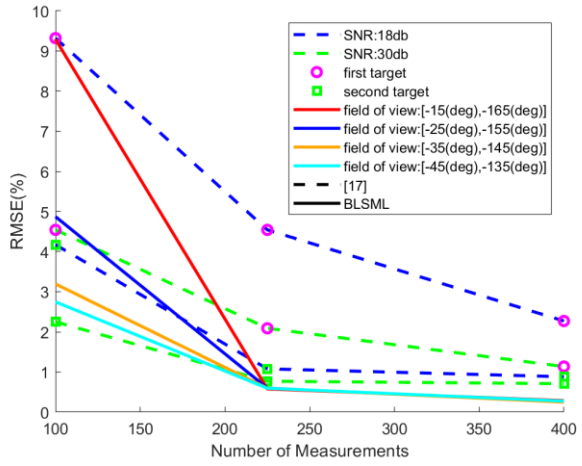

Fig. 7. The evaluation of the proposed method in terms of the number of measurements indicates that the BLSML method outperforms in different FoVs, specifically for measurement counts of 225 and 400.

In Fig. 7., the RMSE values for our proposed method are provided for the number of sensor measurements of 100, 225, and 400, and compared with [17] that the RMSE values are provided for two different SNR values and two different targets. Our proposed method outperforms [17] in terms of performance in the number of sensor measurements of 225 and 400. However, in the case of 100 sensor measurements, [17] has shown better performance.

One of the additional evaluations we conducted for the BLSML method is the CEP assessment. For CEP evaluation, there are two definitions. In the first definition, the 50% error region refers to the area where 50% of the estimated points fall within, and the 90% error region is the area where 90% of the estimated points lie along the drone's traversal path [28]. In the second definition, for each position estimation, an error region can be determined based on the covariance matrix of the estimator [29]. We have utilized the first definition of CEP in this study.

Fig. 8. and Fig. 9. depict the 50% and 90% error regions when the target is at distances of 50 kilometers and 200 kilometers, respectively.

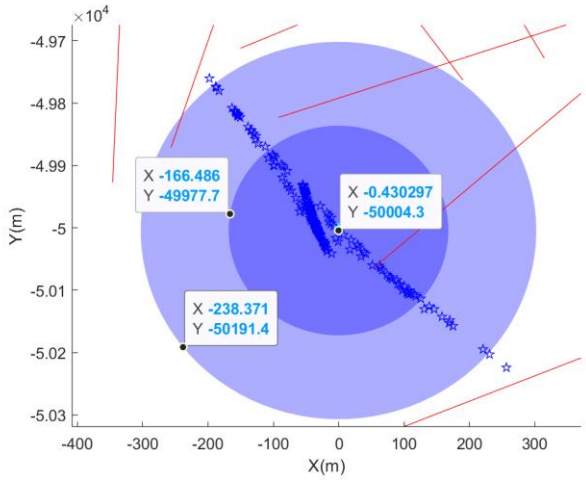

Fig. 8. The 50% and 90% CEP regions. The target was located at a range of 50 kilometers. The radius of the 50% and 90% CEP regions is approximately 168 meters and 302 meters, respectively.

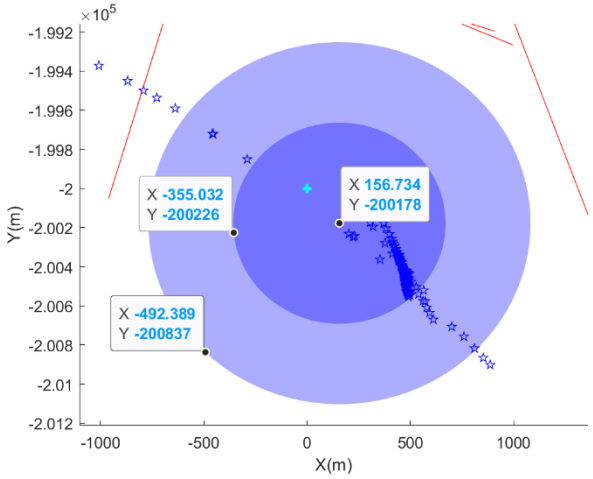

Fig. 9. The target was located at a range of 200 kilometers. The radius of the 50% and 90% CEP regions is approximately 514 meters and 925 meters, respectively.

V. CONCLUSION

The BLSML method, a combination of Brown's LSE and ML techniques, presents a promising approach for accurate target position estimation. By leveraging the advantages of both methods, BLSML offers a robust and efficient solution that can be applied in

practical scenarios. The integration of optimization techniques with the initial estimation process enhances the precision and reliability of target localization. The proposed method has the potential to contribute to various domains, such as military operations, surveillance systems, and navigation applications, where accurate target positioning is crucial.

APPENDIX A

THE CDF OF A GAUSSIAN RANDOM VARIABLE

In order to calculate the CDF of a Gaussian random variable $X \sim N(m.\sigma^2)$, we use the Q function:

$$F_X(x) = \int_{-\infty}^{x} \frac{1}{\sqrt{2\pi\sigma^2}} e^{-\frac{(t-m)^2}{2\sigma^2}} dt = 1 - \int_{x}^{\infty} \frac{1}{\sqrt{2\pi\sigma^2}} e^{-\frac{(t-m)^2}{2\sigma^2}} dt = 1 - \int_{\frac{x-m}{\sigma}}^{\infty} \frac{1}{\sqrt{2\pi}} e^{-\frac{u^2}{2}} du = 1 - Q\left(\frac{x-m}{\sigma}\right) \quad (29)$$

that Q function defined as

$$Q(x) = P\{N(0.1) > x\} = \frac{1}{\sqrt{2\pi}} \int_{x}^{\infty} e^{-\frac{t^2}{2}} dt \quad (30)$$

REFERENCES

1. Poisel, R.A., *Electronic Warfare Target Location Methods*. Second ed. 2012, London: Artech House.
2. Jenkins, H.H., *Small-aperture radio direction-finding*. The Artech House radar library. 1991, London: Artech.
3. Poisel, R., *Introduction to communication electronic warfare systems*. 2002, London: Artech.
4. Neri, F., *Introduction to electronic defense systems*. Second edition. ed. Artech House radar library. 2001, Boston, Mass. ; London: Artech House. xix, 622 pages : illustrations.
5. Van Trees, H.L. and I. NetLibrary, *Optimum array processing*. Detection, estimation, and modulation theory v. 4. 2002, New York: Wiley-Interscience.
6. Cadzow, J.A. *Methods of Direction-of-Arrival*. in *Proceedings IEEE Pacific Rim Conference on Communications, Computers, and Signal Processing*. 1991. IEEE.
7. Cadzow, J.A., *Signal Processing via Least Squares Error Modeling*, in *IEEE ASSP Magazine*. 1990, IEEE. p. 12-31.
8. Golub, G.H., and C. F. Van Loan, *An Analysis of the Total Least-Squared Problem*. SIAM Journal on Numerical Analysis, 1980. **17**: p. 883-892.
9. Pillai, A.P.s.U., *Probability, Random Variables, And Stochastic Processes*. 2002: McGraw-Hill.
10. Brown, R.M., *Emitter Location Using Bearing Measurements from a Moving Platform.* NRL Report 8483, Naval Research Laboratory, Washington, D.C., 1981.
11. Legendre, A., *Nouvelles Methods Pour la Determination des Orbites des Cometes*. 72-75.
12. Poirot, J.L., and M. S. Smith, *Moving Emitter Classification.* IEEE Transactions on Aerospace and Electronic Systems, 1976. **AES-12, No. 2**: p. 255–269.
13. Poirot, J.L., and G. V. McWilliams, *Application of Linear Statistical Models to Radar Location Techniques.* IEEE Transactions on Aerospace and Electronic Systems, 1974. **AES-10, No. 6**: p. 830–834.
14. Jiang, Z.Y.R.W.Y., *A Novel Scheme for Joint Estimation of Velocity, Angle-of-arrival and Range in Multipath Environment*, in *IEEE Global Communications Conference (GLOBECOM)*. 2021, IEEE Global Communications Conference (GLOBECOM): Madrid, Spain.
15. Hiraguri, T.M.S.M.T.M.T., *Performance Improvement of Maximum Likelihood Wave Source Localization with LOS/NLOS Identification*, in *International Conference on Consumer Electronics - Taiwan (ICCE-Taiwan)*. 2023, International Conference on Consumer Electronics - Taiwan (ICCE-Taiwan): PingTung, Taiwan.
16. Liu, X.F.Z.H.J.H.L.S.D., *Single Sensor Emitter Localization Based on TOA Sequence With Inter-Pulse Modulation*, in *IEEE International Radar Conference (RADAR)*. 2020, IEEE International Radar Conference (RADAR): Washington, DC, USA.
17. Al-Dweik, M.A.-J.E.A.A., *Penalized Maximum Likelihood Based Localization for Unknown Number of Targets Using WSNs: Terrestrial and Underwater Environments.* IEEE Internet of Things Journal (Early Access), 2023.
18. Behnia, M.H.R.A.F., *Moving Target Localization in Bistatic Forward Scatter Radars: Performance Study and Efficient Estimators.* IEEE Transactions on Aerospace and Electronic Systems, 2019. **56**(2): p. 1582 - 1594.
19. Seo, H.L.J., *Performance Comparison of Numerical Optimization Algorithms for RSS-TOA-Based Target Localization*, in *IEEE 97th Vehicular Technology Conference (VTC2023-Spring)*. 2023, IEEE 97th Vehicular Technology Conference (VTC2023-Spring): Florence, Italy.
20. McGeehan, B.G.E.M.A.N.J., *A Maximum Likelihood Location Estimator for Non-Line of Sight Geolocation of Radio Emitters*, in *13th European Conference on Antennas and Propagation (EuCAP)*. 2019, 13th European Conference on Antennas and Propagation (EuCAP): Krakow, Poland.
21. Levanon, N., *Interferometry against Differential Doppler: Performance Comparison of Two Emitter Location Airborne Systems.* IEE Proceedings, 1989. **136, Pt. F., No. 2**: p. 70–74.
22. Tran, B.L.T., *Quasi-norm Kernel-based Emitter Localization*, in *55th Asilomar Conference on Signals, Systems, and Computers*. 2021, 55th Asilomar Conference on Signals, Systems, and Computers: Pacific Grove, CA, USA.
23. Manolakis, D.E., and M. E. Cox, *Effect in Range Difference Position Estimation Due to Stations' Position Errors.* IEEE Transactions on Aerospace and Electronic Systems, 1998. **34, No. 1**: p. 328–334.
24. Adamy, D.L., *EW 101 : a first course in electronic warfare*. Radar Library. 2001, Norwood, MA: Artech House.
25. Gavish, M., and Weiss, A., *Performance Analysis of Bearing-Only Target Location Algorithms.* IEEE Transactions on Aerospace and Electronic Systems, 1991. **28. NO. 3**.
26. Salehi, J.P.M., *Digital Communications*. fifth ed.: McGraw-Hill.
27. Gething, P.J.D., *Radio direction finding and superresolution*. IEE electromagnetic waves series 33. 1991, London: Peter Peregrinus on behalf on the Institution of Electrical Engineers. xviii,365p.
28. Adamy, D.L., *EW 102 A Second Course in Electronic Warfare*. 2004: Artech House.
29. Wegner, L.H., *On The Accuracy Analysis of Airborne Techniques For Passively Locating Electromagnetic Emitters*. 1971.